Effects of proton irradiation on luminescence emission and carrier dynamics of self-assembled III-V quantum dots

R. Leon, S. Marcinkevičius, J. Siegert, B. Magness, W. Taylor and C. Lobo

Abstract:

The effects of proton irradiation (1.5 MeV) on photoluminescence intensities and carrier dynamics were compared between III-V quantum dots and similar quantum well structures. A significant enhancement in radiation tolerance is seen with three-dimensional quantum confinement. Measurements were carried out in different quantum dot (QD) structures, varying in material (InGaAs/GaAs and InAlAs/AlGaAs), QD surface density (4×10^{8} to 3×10^{10} cm^{-2}), and substrate orientation [(100) and (311) B]. Similar trends were observed for all QD samples. A slight increase in PL emission after low to intermediate proton doses, are also observed in InGaAs/GaAs (100) QD structures. The latter is explained in terms of more efficient carrier transfer from the wetting layer via radiation-induced defects.

R. Leon is with the Jet Propulsion Laboratory, 4800 Oak Grove Drive, Pasadena, CA 91109
S. Marcinkevicius and J. Siegert are with Department of Microelectronics and Information Technology, Royal Institute of Technology, 100 44 Stockholm, Sweden
B. Magness and W. Taylor are with the Department of Physics and Astronomy, California State University, Los Angeles, CA 90032
C. Lobo is with Cavendish Laboratory, University of Cambridge, Cambridge CB3 0HE, United Kingdom

Introduction:

Semiconductor Quantum dots (QDs) have been the focus of extensive research due to their appealing electronic and optical properties, which have allowed successful implementations of several emerging device applications. QD based devices include novel QD lasers, broadband QD infrared Photodetectors, different types of semiconductor QD memories [1, 2], and highly parallel computing architectures [3] based on quantum dot cellular automata. Recent developments have shown rapid progress in the implementation of some of the advantages of QD based lasers predicted by theory [4] demonstrating reductions in threshold-current densities [5,6] and an order of magnitude lower chirp [7]. Likewise, QD based infrared photodetectors have shown broader band absorption, and the ability of incident light absorption expected from the different selection rules between QDs and QWs [8].

Protons can cause displacement damage and structural defects in semiconductor devices, resulting in performance degradation and failure. Minimizing the impact of radiation-induced degradation in optoelectronic devices is therefore important for several applications, and it can include the exploitation of inherent radiation hardness in quantum structures. Some of the fundamental properties of QDs suggest that optoelectronic devices incorporating QDs could tolerate greater radiation damage than other heterostructures. Exciton localization in the quantum dots due to three-dimensional confinement reduces the probability of carrier non-radiative recombination at radiation induced defect centers if damage is created outside the QD region. Recent findings show that indeed, some types of semiconductor quantum dots QDs are very radiation hard, which makes some QD based optoelectronic devices ideal for space applications. Recent studies of optical properties in proton, ion, and electron-irradiated quantum dot (QD) structures [9-11] and in ion, and proton-irradiated QD lasers

[12,13] showed that the QDs structures and QD based devices are much more resistant to radiation induced damage than bulk semiconductors or quantum wells (QW). Some of these studies showed not only better radiation tolerance, but also an increase in either photoluminescence (PL) intensities [9] or laser performance [11] with low proton or ion fluences. A better understanding of the physical processes responsible for this surprising finding was one of the aims of this present work. In order to accomplish such understanding, comparisons of optical emission intensities and carrier dynamics from different types of III-V Quantum Dots and Quantum Wells (QW) after irradiation with 1.5 MeV protons were undertaken. Results presented here confirm better radiation tolerance from all the QDs studied, and give insights into the mechanisms for higher PL intensities after radiation exposure observed in some of the QD structures.

Experimental details:

InGaAs/GaAs (100), InAlAs/AlGaAs (100) and InGaAs/GaAs (311)B QDs were grown by metal-organic chemical-vapor deposition in a horizontal reactor cell operating at 76 Torr. Trimethylgallium, trimethylindium, trimethylaluminum (for growth of InAlAs and AlGaAs) and arsine were used as precursors. For the InGaAs QDs, growth of a 50 nm GaAs buffer layer at 650°C was followed by deposition of 1.5 nm InGaAs with a nominal indium mole fraction of 0.6. Different surface densities of InGaAs QDs in similar sizes were obtained by changing the arsine partial pressures during growth of the QDs [14]. InGaAs quantum wells (QWs) were obtained by stopping the growth of InGaAs before the onset of the Stranski-Krastanow transformation, giving thin (1 nm) QWs. For the InAlAs/AlGaAs QDs, growth of a 500 nm AlGaAs buffer layer at 775°C and nominal Aluminum mole fraction of 0.35 was followed by deposition of 1.5 nm InAlAs with

nominal indium mole fraction of 0.55. InGaAs and InAlAs QDs were capped with 100 nm GaAs (AlGaAs) layers, deposited while the temperature was gradually raised to 600 (700)°C. When AlGaAs barriers were used, a final 10 nm GaAs capping layer was deposited to prevent surface oxidation. Atomic force microscopy and transmission electron microscopy were used to give information on island sizes and surface densities in capped and uncapped InGaAs and InAlAs QDs. Proton irradiations were carried out using a Van De Graaff accelerator. Samples were irradiated at room temperature using 1.5 MeV protons at five different doses ranging from 1.3×10^{11} to $3.5 \times 10^{13}/cm^2$, with a dose rate ~ 6×10^{12} protons/sec. Dose uniformity was monitored using radiochromic film at low doses. Carrier dynamics were studied by time-resolved photoluminescence (PL) at 80 K after excitation by a short laser pulse from a self mode-locking Ti:saphire laser (pulse duration 80 fs, repetition frequency 95 MHz). The excitation wavelength was 800 nm for the InGaAs structures and 400 nm for the InAlAs QDs. For the PL detection either an upconversion set-up with a temporal resolution of 150 fs or a synchroscan streak camera with an infrared enhanced photocathode, combined with a 0.25 m spectrometer (temporal resolution 3 ps) were used. Ternary compositions [$In_{0.6}Ga_{0.4}As$, $In_{0.55}Al_{0.45}As$, and $Al_{0.35}Ga_{0.65}As$] between QWs and QDs were identical, and so were capping layer thicknesses (100 nm for both QDs and QWs), therefore these results are not dependent on material or proton energy loss differences.

Results from experiments and simulations:

Table 1 presents a summary and description of the different structures used in this study, showing their materials and structural properties (dot sizes, aspect ratios and concentrations) as well as the wavelength emission at their PL maximum intensity. It can

be seen that the emission from the InGaAs QW is at a higher energy than from the InGaAs QDs. This is because very thin QWs (1 nm) are used to obtain a strained QW of the same ternary composition as the QDs but without dislocations. It is worth noting that InGaAs/GaAs(311)B QDs have similar diameters, but form in slightly higher surface concentrations with lower aspect ratios than InGaAs/GaAs(100) QDs. Since the dimensions in the growth direction dominate quantum confinement energies, corresponding PL emission peaks are also at higher energies [15]. As shown from the values in this table, the high density InGaAs QDs exhibit a blueshift of the PL emission energy with respect to the low density InGaAs QDs. These differences are not seen to correspond to variations in dot sizes or compositions, and have been ascribed to strain deformation of the QD confining potentials, resulting in shallower effective confinement with increasing dot density [16].

Figure 1 shows the dependence of the peak PL intensity on proton fluences for the QD and the QW samples. The difference between the QWs and QDs is striking: At the highest proton fluence, the QW PL intensity is ~30 times lower than for the unirradiated sample, while the QD PL intensity decreases to just a little over half of its original intensity. Moreover, as observed in earlier work [9], we observe an *increase* in the QD PL intensity for the (100) InGaAs/GaAs QDs (most prominent, up to 50%, in the low-density dots) for small irradiation doses as compared to the un-irradiated QDs.

Fig. 2 shows a comparison of two spectra illustrating the effects of 1.5 MeV proton irradiation in low surface density QD structures. These structures show a bright emission from the wetting layer (WL) seen here at above 1.3 eV. In the growth of these InAs-InGaAs/GaAs and InAlAs/AlGaAs quantum dots, a two dimensional layer is first formed on

the barrier layer. After a certain strain dependent critical thickness is reached, typically 2-6 mono atomic layers, islands form spontaneously in what is known as the Stranski-Krastanow transformation. These islands are of nanometer dimensions, and they also have good size calibration. After formation of these islands, the pre-existing two-dimensional "wetting layer" remains under the islands or QDs. The surface density of these QDs can be varied, either by stopping the growth before saturation island density is reached [17], or by using growth conditions that maximize the surface energy of the growth layer [14]. If the average QD separation is greater than the photocarrier diffusion lenghts, recombination from WL states will ocur for photocarriers generated in the WL, and a PL peak from the WL will be observed. The WL behaves as a reservoir of carriers that become available to the dots as long as the 2D diffusion length in the WL is large enough for capture to be possible, and as long as capture occurs before radiative recombination from WL states. Fig. 2 shows that proton irradiation has different effects in the two-dimensional structures (WL peak at 1.3 eV) than in the zero-dimentional structures (QD peak showing excited states emission, 1.1 eV for ground state).

Figure 3 shows the PL transients for one of the samples (high surface density InGaAs/GaAs (100) QDs), presented as a function of increasing proton fluence. After a fast rise with a characteristic time of 4 –5 ps (not resolved in Fig. 3), the PL decays due to both radiative and nonradiative carrier recombination. The dependence of the PL decay times on proton fluence is shown in Figure 4 for all the infrared-emitting samples. As shown in Fig. 4, carrier lifetimes in QDs are less affected by proton irradiation than in the QWs. For example, the 80 K carrier lifetimes in (311)B QDs decrease from 2.2 ns for the

unirradiated sample to 1.4 ns for the sample with the highest proton dose, compared to a ~20-fold and ~40-fold decrease for the QW and the WL, respectively.

Fig. 5 shows the variations in QD PL rise times for all QD samples, also as a function of increasing proton fluence. It can be seen that QD PL rise times, which reflect carrier capture from the barriers into the dots, decrease with irradiation.

Figure 6 shows the expected Ranges of Hydrogen ions (protons) in GaAs calculated from "Trajectories and Ranges of Ions in matter (TRIM)" [18] simulations. Also shown, are the calculated numbers of total target displacement events per ion per Angstrom at a depth of 100 nm in GaAs. An inverse relation between range and displacement defects created can be seen.

Fig. 7 shows PL dynamics for the visibly emitting InAlAs/AlGaAs QDs. Unlike in the other QD samples, two different exponentials are needed to obtain a good fit for the PL decay times. The behavior of the long and short PL decay time components is shown in the inset as a function of proton fluence.

Additional continuous wavelength (CW) PL experiments were performed on InGaAs (100) QDs by varying the energy of optical excitation. In this experiment, the goal was to use two different excitation wavelengths (energies), so photoexcitation of carriers in the WL was achieved at 920 nm (1.348 eV), and as the wavelength was tuned to 970 nm (1.278 eV) carriers were excited only in the QDs. This experiment allows differentiation between carriers generated in the WL and showing changes in the transfer process into the QDs, and changes in PL decay times for carrier photoexcited directly into the QDs. When 920 nm excitation was used, a similar PL intensity increase was observed as in the case of

above bandgap excitation (similar to what is shown in Fig. 1), while for excitation in the dots the PL intensity for moderate irradiation fluences was irradiation-independent.

Discussion:

As can be seen, PL intensities and carrier lifetimes in QDs are much less affected by proton irradiation than in the QWs (or the WL in the low-density QD structures), which implies that InGaAs QDs are more radiation tolerant than QWs of the same composition. This increase in radiation hardness is significant, because QW based devices already represent a vast improvement in radiation hardness over bulk devices. For example, experiments performed with 50 MeV protons on different types of light emitting diodes (LEDs) used in optocoupler applications, showed significantly worse degradation for the pn junction based amphoterically doped (Si) GaAs LEDs than for the GaAs/AlGaAs LEDs based on QWs (also known as double-heterojunction LEDs) [19, 20]; these studies demonstrated that LEDs based on QWs showed over an order of magnitude greater tolerance to proton induced displacement damage when compared to the LEDs based on pn junction geometries. An important difference for the QD and QW comparison here, is that unlike the case reported for the LED study (20), the initial emission from the QDs is stronger than from the QWs, so initial brightness is not compromised in device applications.

A rough comparison between the present results and the cited earlier studies can be made using the calculated ratios of displacement events per ion per Angstrom at the known active region depth shown in Fig. 6, which shows that at a depth of 100 nm in GaAs, 1.5 MeV protons cause ~ 25 times more damage than 50 MeV protons. Since this damage ratio is an estimation, further experiments at higher proton energies should also be performed in

some of these QD and QW structures for greater accuracy and in order to eliminate unforseen effects.

Similar trends are observed for all QD samples, and can be explained by the different level of confinement in the QW and QD structures. These observations can be explained if we consider that unlike in QWs, carriers in QDs are not mobile and their lifetime is reduced only by the defects created inside the dots. In the QW structures, the carriers are mobile in the QW plane therefore they can easily find a trap and be rapidly removed from the conduction/valence bands. On the other hand, carriers in the QDs are confined in all three dimensions and are not mobile. Only defects created inside the QDs contribute to reduction of the carrier lifetime.

The measured dependence of the PL decay time on irradiation dose can be used to evaluate trapping rates to the native and radiation-induced defects. The full line in Fig. 4 corresponds to the relation $\tau = 1/(B_0 + B_i)$, where τ is the PL decay time and B_0 and B_i are carrier trapping coefficients to the native and irradiation-induced centers, respectively. In the as-grown QW sample the PL decay time is 500 ps. This time is mostly determined by the nonradiative recombination (the radiative recombination time in InGaAs/GaAs QWs at 80 K is of the order of nanoseconds [21]). Considering that in the 1 nm thin QW most of the electron wave function is spread into the barriers [22], carrier lifetime in the thin QW is mainly determined by traps within the barriers. The main electron traps in MOCVD grown GaAs are ionized EL2 donors [23]. This trap concentration can be evaluated from the known EL2 electron capture cross-section [23] and the PL decay time measured in the QW sample, which gives a native trap concentration of $\sim 2\times10^{15}$ cm^{-3}. This simple model describes the experimental results rather well, and it shows that at

proton fluences of 1×10^{12} cm^{-2}, the trapping rates to the native and radiation-induced defects are equal.

A comparison between these values and the estimated radiation induced defect centers obtained from the fit of the experimental data on PL decay times is now possible, and it shows some interesting findings. Fig. 6 shows that 2×10^{-5} displacement defects are created per each energetic ion (proton) per each angstrom depth in the vicinity of 100 nm depth in GaAs. In order to interpret these results and reconcile them with the fit shown in Fig. 4, it must be taken into account that the light output or PL intensity from the QW will be affected by defects created within the well, and outside the well area, since electron hole recombination will limit carrier transfer to the QW.

It is well known that proton irradiation in GaAs produces a wide spectrum of displacement defects including As antisites (EL2), As vacancies, and As vacancy – interstitial complexes [23, 24]. Ionized EL2 defects are considered to be the main electron traps in proton-irradiated samples [25]. Moreover, other electron traps, such as E4, present at concentrations comparable to that of EL2 in proton irradiated samples [23,24], have similar electron capture cross sections as the EL2. The same or similar origin of traps and capture cross sections in as-grown and irradiated QW samples allow us to make an estimation of irradiation-induced defect concentration. For proton fluence of 1×10^{12} cm^{-2} when the capture coefficients to the native and induced defects are equal, the irradiation-related active trap concentration should be of the order of 10^{10} cm^{-2}. This result shows that about one in one hundred (1/100) protons induces electron traps in the vicinity of the thin QW.

The decrease in QD PL rise times seen in Fig. 5 is mainly attributed to the reduction of carrier transport time (due to carrier trapping to defects) in the barriers, from which the carriers are collected into the QDs. The shorter capture times and lower total PL intensities simply reflect the fact that QDs collect only carriers generated closer to the dots, since electron-hole pairs excited further away from the QDs can recombine non-radiatively at radiation-induced defect centers.

The remarkably small decrease in PL peak intensities for InAlAs QDs shown in Fig. 3 and the small effect of proton irradiation on their PL decay times shown in Fig. 4 demonstrate that when other impurity-related defects are present in QD structures, additional defects introduced by irradiation have a very little effect on the PL intensities and QD carrier dynamics, which make these QD structures even more radiation tolerant.

Regarding the origin of the double exponential decay times observed for the InAlAs quantum dots shown in Fig. 7; one is determined by trapping of one type of carriers (electrons or holes) to defect centers, the longer one reflects carrier recombination. In the unirradiated InAlAs QDs, contrary to the InGaAs structures, the carrier lifetimes are governed not by the radiative recombination but by unintentional impurities incorporated in the sample during growth. This interpretation is supported by the shorter PL decay times reported here and by measurements of the temperature dependence of the PL emission, which gave low values (E_a = 88 meV) for the activation energy for quenching of the PL emission for these InAlAs dots [26]. This is much lower than the QD confining potentials ($E_B - E_{QD}$ = 200 meV).

The surprising enhancement of the PL intensity from QD structures seen at low to intermediate proton fluences can been explained by two possible mechanisms:

i. Reduction of the phonon bottleneck by defect assisted phonon emission has been proposed [27] as a mechanism to explain the bright PL emission in QDs. Perhaps in dots with defect free interfaces, introduction of deep level defects as those originated from displacement damage might provide additional relaxation paths [28] for thermalization of carriers and therefore increase the luminescence emission.

ii. Several recent experiments have identified capture barriers (also known as potential or energy barriers) at the QD/barrier interface [29-31]. These barriers are attributed to strain effects and have been shown to affect or inhibit carrier transfer into the quantum dots. If irradiation-created defects near the QD/barrier interface, where the potential barriers have been identified, affect the efficiency of carrier transfer into the QDs, PL emission from QD states would increase. Increased carrier collection from the WL to the QDs may occur due to an additional channel of carrier transfer, namely, trapping via radiation-induced defects. During such a process, carriers are first trapped from the WL into defect levels, relax and tunnel into the dots.

The results presented here allow an unambiguous determination of which is these two mechanisms prevails and can best explain the observed PL intensity increase seen after fluences ~ 10^{11} and 10^{12} protons/cm^2. Elucidation of the physical mechanism responsible for this unusual PL increase can be achieved by examination of the data presented in Fig. 1 and Fig. 4; as well as from the PL intensity measurements performed using laser excitation at wavelengths above the WL energy and below the WL energy (at 920 nm and 970 nm).

If the observed PL increase is due to the first mechanism proposed (i), then we should observe:

(a) An increase in PL lifetime (longer decay times) at the same proton fluences that show a PL increase with above bandgap excitation, and;

(b) A similar increase in PL intensity with low to intermediate proton fluences when using excitation energies below the WL energy.

Since neither (a) nor (b) are observed, our results suggest rather, an increase in the efficiency with which the carriers are transferred into the QDs. As previously reported [29, 30], capture into the dots may be inhibited by strain-induced potential barriers at the QD/WL interfaces. Increased carrier collection from the WL to the QDs may occur due to an additional channel of carrier transfer, namely, trapping via radiation-induced defects. During such a process, carriers are first trapped from the WL into defect levels, relax and tunnel into the dots. Here we should note that these defects should have shallower energy levels (with a confinement energy less or equal to that of a dot) compared to the defects discussed above. A possible candidate is the level E2, formed by an As vacancy and an interstitial [25]. For the tunneling process to be efficient, a defect should be situated within 20 nm from the QD [27]. If we assume that the density of these shallower levels is similar to that of the deeper defects, the average distance between randomly distributed defects for the 1×10^{12} cm^{-2} irradiation dose is around 100 nm. This is too low for each dot to have an accompanying defect, however, such defects might still be important for the enhanced carrier transfer into some of the dots. Further experiments that allow more detailed characterization of the energies, concentrations, and capture cross-sections of the

radiation-induced defects introduced in the vicinity of the QDs will allow further understanding of this proposed mechanism.

Conclusions:

In summary, comparison of PL intensities and decay times between QWs and various types of III-V quantum dots after 1.5 MeV proton irradiation show an increase in radiation hardness of as much as two orders of magnitude in quantum dots. We have observed that carrier lifetimes in QDs are not strongly affected by displacement damage defects introduced by proton irradiation. This can be explained by better carrier localization in the QDs than in QWs. Enhancement of the PL intensity at low to moderate radiation doses suggests a more effective carrier transfer from the WL into the QDs after irradiation. This may occur due to an additional channel of carrier trapping from the barriers and the WL into the QDs, namely, trapping from the WL to the QDs via radiation-induced defects.

Acknowledgments:

Part of this research was carried out at the Jet Propulsion Laboratory, California Institute of Technology, under a contract with the National Aeronautics and Space Administration. Financial support from the Swedish Foundation for International Cooperation in Research and Higher Education (STINT) is gratefully acknowledged.

REFERENCES:

1. S. Muto, *Jpn. J. Appl. Phys.* **34**, L210 (1995).
2. M. Shima, Y Sakuma, T Futatsugi, Y Awano, and N Yokoyama, *IEEE Trans. Electron Devices* **47**, 2054 (2000).
3. A. O. Orlov, I. Amlani, G. Toth, C. S. Lent, G. H. Bernstein, G. L. Snyder, *Appl. Phys. Lett.* **74**, 2875 (1999).
4. Y. Arakawa and H. Sakaki, *Appl. Phys. Lett.* **40**, 939 (1982).
5. G. Park, O. B. Shchekin, D. L. Huffaker, and D. G. Deppe, *IEEE Photonics Technol. Lett.* **12**, 230 (2000).
6. X. Huang, A. Stintz, C. P. Hains, G. T. Liu, J. Cheng, and K. J. Malloy, *Electron. Lett.* **36**, 41 (2000).
7. H. Saito, K. Nishi, A. Kamei, and S. Sugou, *IEEE Photonics Technol. Lett.* **12**, 1298 (2000).
8. H. C. Liu, M. Gao, J. McCaffrey, Z. R. Wasilewski, and S. Fafard, *Appl. Phys. Lett.* **78**, 79 (2001).
9. R. Leon, G. M. Swift, B. Magness, W. A. Taylor, Y. S. Tang, K. L. Wang, P. Dowd, and Y. H. Zhang, *Appl. Phys Lett.* **76**, 2074 (2000).
10. W. V. Schoenfeld, C. H. Chen, P. M. Petroff, and E. L. Hu, *Appl. Phys. Lett.* **73**, 2935 (1998).
11. N. A. Sobolev, A. Cavaco, M. C. Carmo, M. Grundmann, F. Heinrichsdorff, and D. Bimberg, *Phys. Stat. Solidi B* **224**, 93 (2001).

12. P. G. Piva, R. D. Goldberg, I. V. Mitchell, D. Labrie, R. Leon, S. Charbonneau, Z. R. Wasilewski, and S. Fafard, *Appl. Phys Lett.* **77**, 624 (2000).

13. C. Ribbat, R. Sellin, M. Grundmann, D. Bimberg, N. A. Sobolev, and M. C. Carmo, *Electron. Lett.* **37**, 174 (2001).

14. R. Leon, C. Lobo, J. Zou, T. Romeo, and D. J. H. Cockayne, *Phys. Rev. Lett.* **81**, 2486 (1998).

15. C. Lobo, N. Perret, D. Morris, J. Zou, D. J. H. Cockayne, M. B. Johnston, M. Gal, and R. Leon, *Phys. Rev. B* **62**, 2737 (2000).

16. R. Leon, S. Marcinkevičius, X. Z. Liao, J. Zou, D. J. H. Cockayne, and S. Fafard, *Phys. Rev. B* **60**, R8517 (1999).

17. R. Leon and S. Fafard, *Phys Rev.* ***B*** **58**, R1726 (1998).

18. http://physics.nadn.navy.mil/physics/Faculty/Ziegler/home.htm

19. B. G. Rax, C. I. Lee, A. H. Johnston, and C. E. Barnes, *IEEE Trans. Nucl. Sci.* **43**, 3167 (1996).

20. A. H. Johnston, B. G. Rax, L. E. Selva, and C. E. Barnes, *IEEE Trans. Nucl. Sci.* **46**, 1781 (1999).

21. H. Yu, C. Roberts, and R. Murray, *Mat. Sci. Eng.* **B35**, 129 (1995).

22. P. Borri, W. Langbein, and J. M. Hwam, *Phys. Rev. B* **59**, 2215 (1999).

23. H. H. Tan, J. S. Williams, and C. Jagadish, *J. Appl. Phys.* **78**, 1481 (1995).

24. F. H. Eisen, K. Bachem, E. Klausman, K. Koehler, and R. Haddad, *J. Appl. Phys.* **72**, 5593 (1992).

25. R. Ferrini, M. Galli, G. Guizzetti, M. Patrini, F. Nava, C. Canali, and P. Vanni, *Appl. Phys. Lett.* **71**, 3084 (1997).

26. C. Lobo, Ph.D. dissertation, Australian National University, March 2000.

27. P. C. Sercel, *Phys. Rev. B* **51**, 14532 (1995).

28. H. Benisty, C. M. Sotomayor-Torres, and C. Weisbuch, *Phys. Rev. B* **44**, 10945 (1991).

29. C. Lobo, R. Leon, S. Marcinkevičius, W. Yang, P. C. Sercel, X. Z. Liao, J. Zou, and D. J. H. Cockayne *Phys. Rev. B* **60**, 16647 (1999).

30. S. Marcinkevičius and R. Leon, *Appl. Phys. Lett.* **76**, 2406 (2000)

31. H. L. Wang, F. H. Yang, S. L. Feng, H. J. Zhu, D. Ning, H. Wang, and X. D. Wang, *Phys. Rev. B* **61**, 5530 (2000).

Table 1. Data summary for QDs and QW structures used in this study.

Structure and material dot/barrier	Surface density (in dots/cm^2)	Average diameter (nm)	Average aspect ratio (height/diameter)	80 K PL peak energy (eV)
InGaAs/GaAs quantum well	_____	1 nm width	_____	1.35
Low density InGaAs/GaAs (100) QDs	4×10^8	25 ± 5	1/6	1.06 (ground state)
High density InGaAs/GaAs (100) QDs	2×10^{10}	25 ± 5	1/6	1.18
InGaAs/GaAs (311)B QDs	3×10^{10}	25 ± 5	1/8	1.32
InAlAs/AlGaAs (100) QDs	1×10^{11}	20 ± 5	1/6	1.82

Figure Captions:

Figure 1. Changes in PL peak intensities shown for different QD structures and for thin InGaAs QW as a function of proton fluence, shown in (a) linear, and (b) logarithmic scales.

Figure 2. Comparison of initial (solid line) and post irradiation (dotted line) PL spectra at a proton dose 2.7 x 10^{12}/ cm^2 of low density InGaAs/GaAs QDs (3.5 x 10^8 dots per cm^2). The spectra were obtained at constant excitation and show simultaneous emission form QD and wetting layer states.

Figure 3. PL intensity vs. time for high surface density InGaAs QDs for different proton (1.5 MeV) fluences. The PL decay times shown in figure 3 are extracted from single exponential fits of Fig. 2 (and analogous plots).

Figure 4. PL decay times for all infrared-emitting QD structures and InGaAs QW as a function of varying proton fluence. Solid line is fit for QW using the relation……..

Figure 5. PL rise times for all QD structures vs. proton fluence.

Figure 6. Calculated ranges in GaAs for 1.5 MeV protons (solid symbol); and calculated displacement defects per ion per Angstrom at a depth of 100 nm in GaAs (hollow symbols) as a function of proton beam energy.

Figure 7. PL transient with double-exponential decay for InAlAs/AlGaAs QDs after 1.5 meV proton irradiation at a dose of 6.9 $\times 10^{12}$ cm^{-2}. The PL dynamics show the same qualitative behavior even prior to irradiation. The inset shows the behavior of the long and short decay time components with varying proton dose.

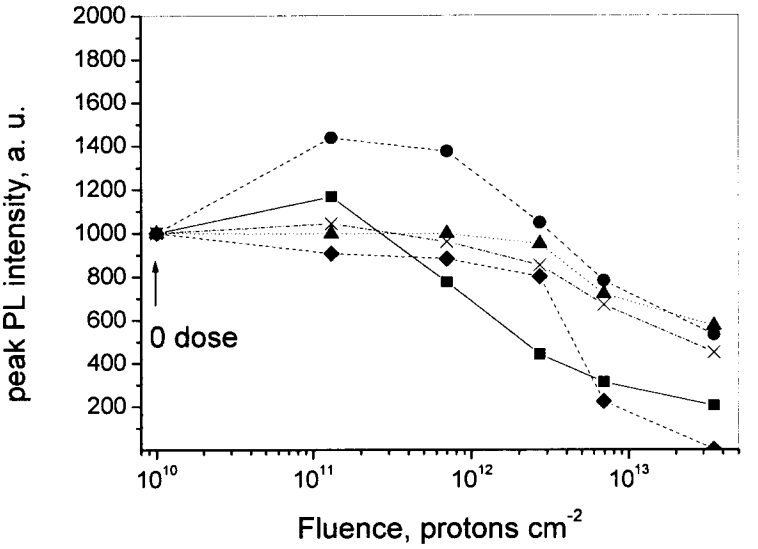

(a)

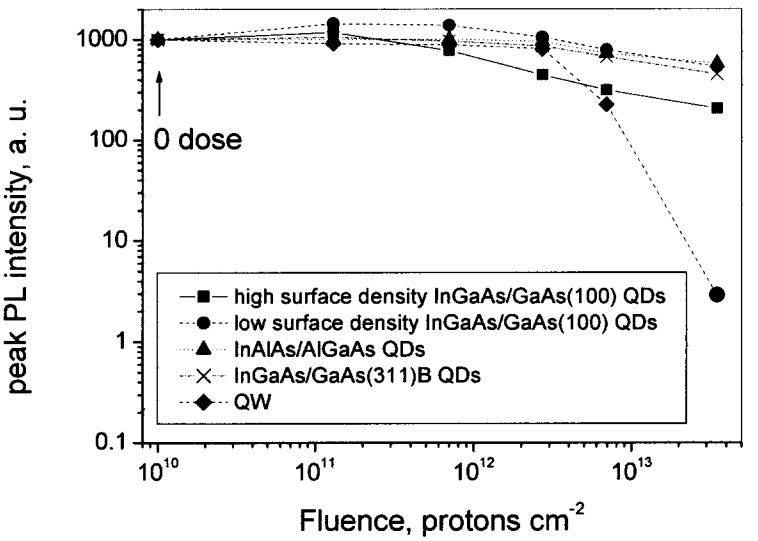

(b)

Figure 1, R. Leon et al.

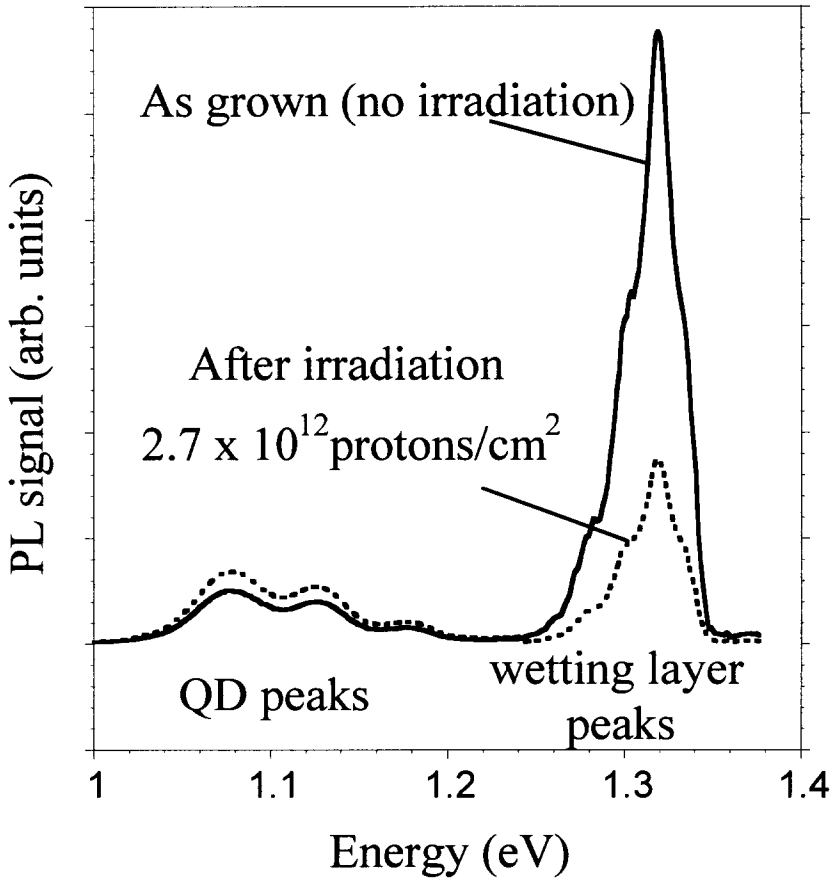

Figure 2, R. Leon et al.

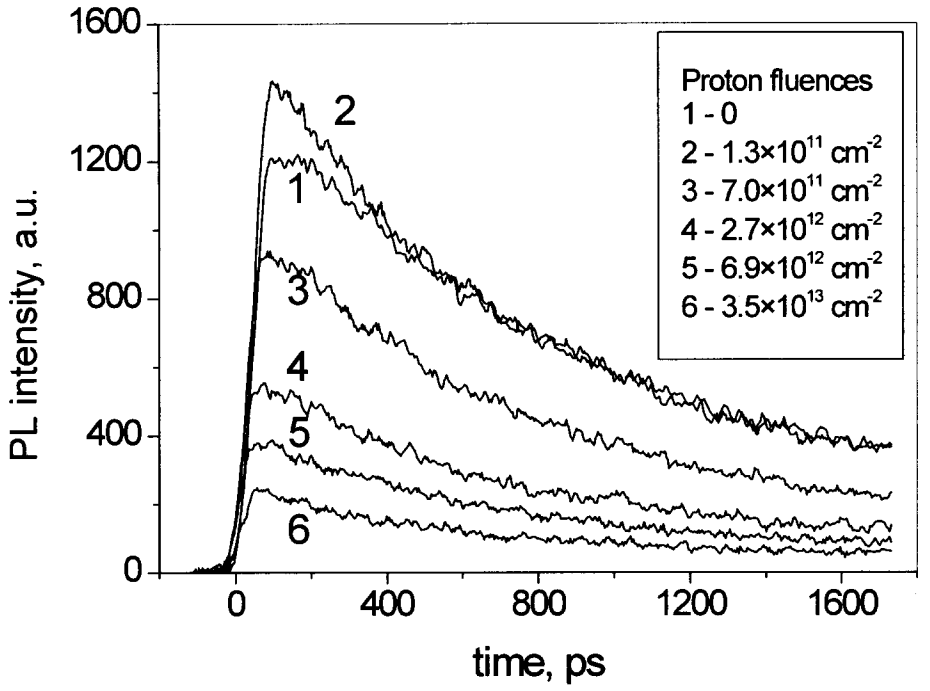

Figure 3, R. Leon et al.

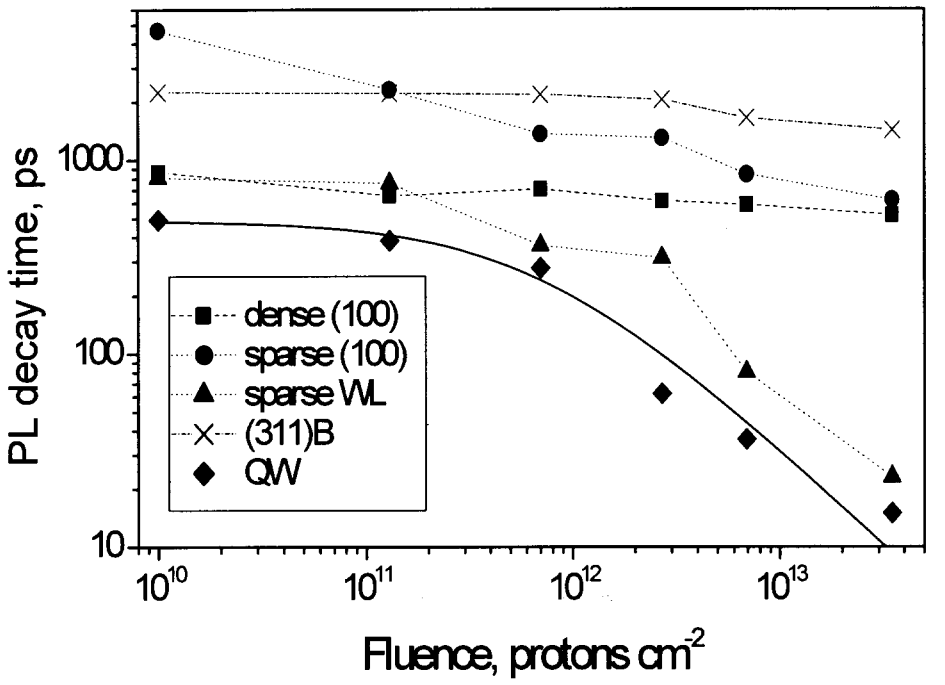

Figure 4, R. Leon et al.

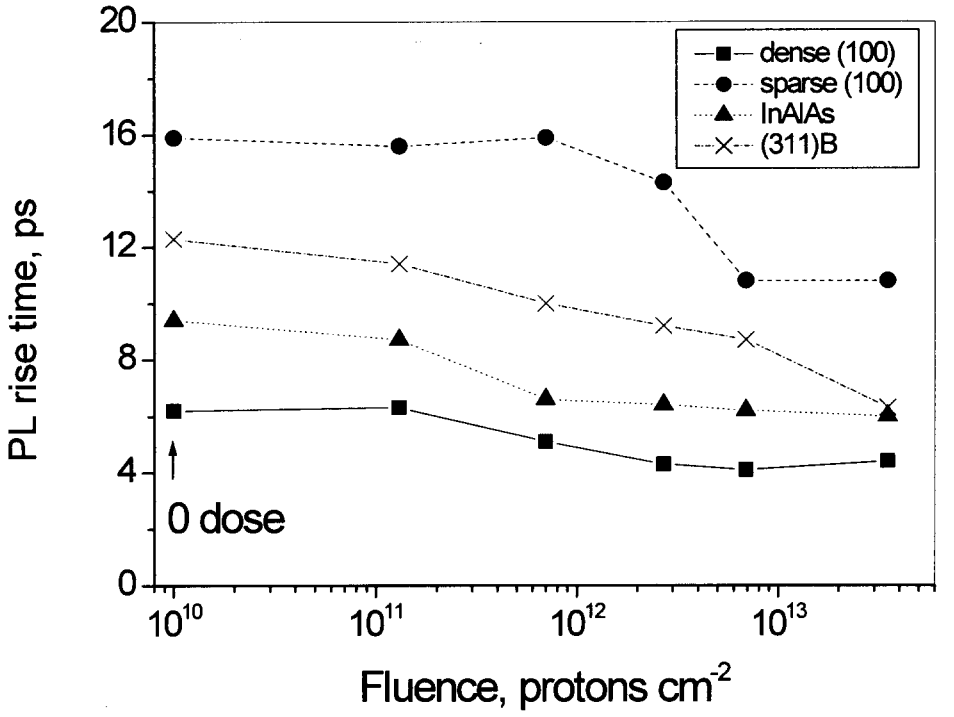

Figure 5, R. Leon et al.

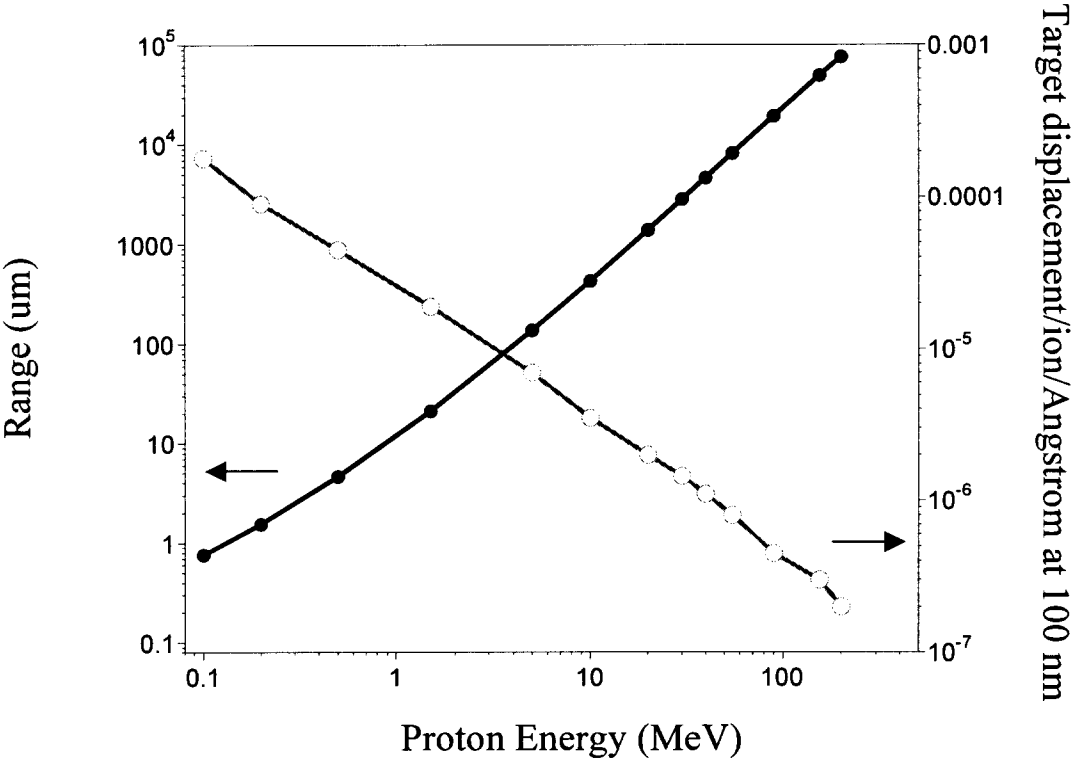

Figure 6, R. Leon et al.

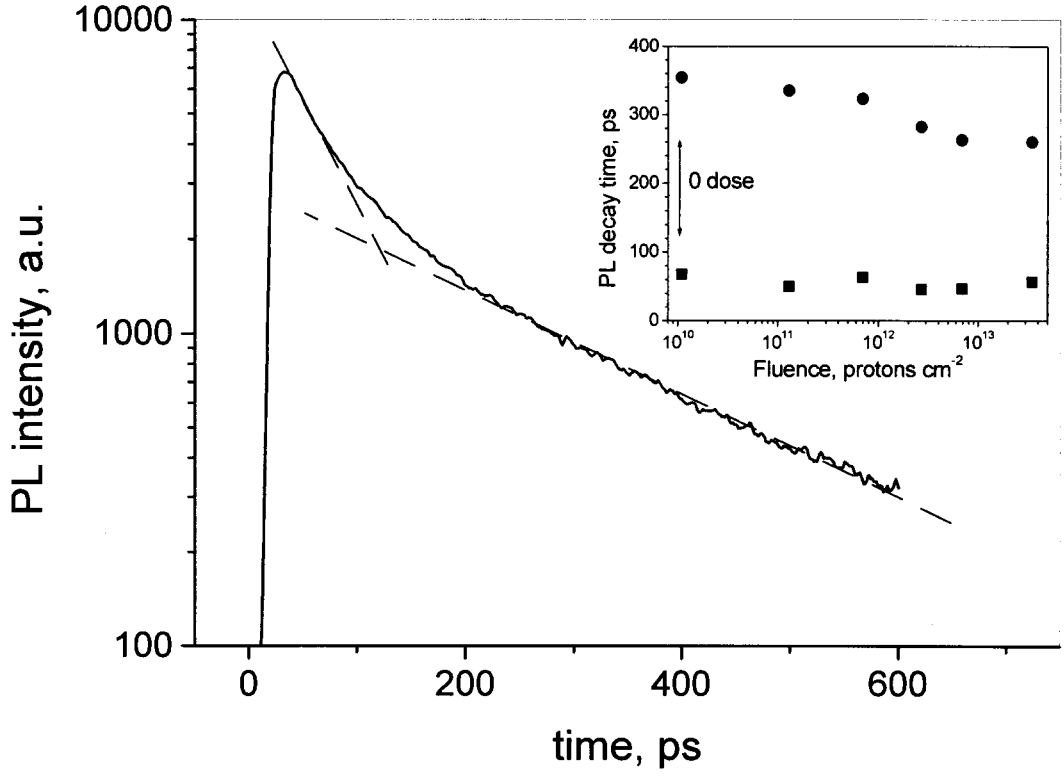

Figure 7, R. Leon et al.